Supporting information

Simultaneous assistance of molecular oxygen/mesoporous SO$_3$H-alumina for a selective conversion of biomass-derived furfural to γ-valerolactone without an external addition of H$_2$

Surachai Karnjanakom [a*], Asep Bayu [b], Panya Maneechakr [a], Chanatip Samart [c], Suwadee Kongparakul [c], Guoqing Guan [d]

[a] Department of Chemistry, Faculty of Science, Rangsit University, Pathumthani 12000, Thailand

[b] Research Center for Biotechnology, Indonesian Institute of Sciences (LIPI), Jalan Raya Jakarta-Bogor KM. 46, Cibinong, Bogor, West Java, Indonesia.

[c] Department of Chemistry, Faculty of Science and Technology, Thammasat University, Pathumthani 12120, Thailand

[d] Energy Conversion Engineering Laboratory, Institute of Regional Innovation (IRI), Hirosaki University, 2-1-3, Matsubara, Aomori 030-0813, Japan

*Corresponding author.

E-mail addresses: surachai.ka@rsu.ac.th and surachaikarn@gmail.com (S. Karnjanakom)

1. Experimental

1.1. Catalyst Characterization

1.1.1. Surface area and porosity measurements

The textural properties of as-prepared catalyst including surface area, pore volume and pore size were analyzed via N_2 adsorption-desorption isotherms using a Quantachrome Autosorb 1 gas analyzer. Before measurement, the catalyst powder was pretreated at 120 °C for 6 h to eliminate the moisture and some organic impurities within the catalyst structure. The surface area and porosity of catalyst were determined by Brunauer–Emmett–Teller (BET) and Barrett–Joyner–Hallenda (BJH) methods, respectively.

1.1.2. X-ray diffraction (XRD)

The X-ray diffraction (XRD) patterns were applied to confirm the type of alumina structure which recorded using an X-ray diffractometer (Rigaku TTRAX III) in 2 theta range of 10-80° with a scanning step of 0.02° at each point using Cu Kα (λ=0.15418 nm) radiation at 40 kV and 20 mA.

1.1.3 Transmission electron microscopy (TEM) and Scanning electron microscopy- Energy dispersive spectroscopy (SEM-EDS)

The 2D and 3D morphologies of catalyst and the presence of S and Al elements on catalyst were observed by a transmission electron microscope (TEM), a scanning electron microscope equipped with energy dispersive spectroscopy (EDS). Before the SEM-EDS observation, the dried catalyst powder was dried in vacuum oven at first, and then dispersed on carbon tape supported on stub. To obtain SEM image with higher resolution, it was further pretreated by Pt sputtering. In case of TEM, the sample was sonicated in ethanol for approximately 10–15 min, and then dropped on a copper grid and dried at room temperature

1.1.4. Fourier transform infrared spectrometry (FT-IR)

The existence of sulfonic group on catalyst was verified by Fourier transform infrared spectrometry (FT-IR) using a PerkinElmer Spectrum 100 FT-IR spectrometer with attenuated total reflectance (ATR) techniques at the range of wavenumber between 4000 and 500 cm^{-1}. Before FT-IR measurement, the catalyst powder was derided at 110 °C to remove moisture adsorbed inside structure.

1.1.5. X-ray photoelectron spectroscopy (XPS)

The surface electronic states of catalyst including of Al 2p, S 2p and O 1s were analyzed by X-ray photoelectron spectroscopy (XPS, Thermo VG ESCALAB250 using AlKa radiation). Prior to the XPS measurements, the catalyst was pretreated in a 10 vol% H_2/Ar flow at 180 ˚C for 4 h. The XPS data were internally calibrated by fixing the binding energy of C 1s at 284.6 eV.

1.1.6. Thermogravimetric analysis (TGA)

Thermal stability of sulfonic group functionalized on catalyst and humins amount adsorbed on spent catalyst were investigated using a Thermogravimetric analyzer (Mettler Toledo TGA/SDTA 851). Analysis process was conducted from temperatures of 100-700 °C using O_2 gas at a flow rate 10 ml/min with a heating rate 5 °C/min.

1.1.7. NH₃-Temperature-programmed desorption (NH₃-TPD)

The catalyst acidity was determined by NH_3-Temperature-programmed desorption (NH_3-TPD) using a TPR/TPD/TPO analyzer. Before measurement, the catalyst powder was preheated at 350 °C for 2 h under He flow (50 ml/min) in order to remove the moisture and some organic impurities inside the catalyst structure. For NH_3 adsorption procedure, the NH_3 gas (5% of NH_3/He) was adsorbed on catalyst at 40 °C for 1 h with a flow rate of 50 ml/min until it was saturated. Thereafter, NH_3 desorption process was carried out by increasing of temperature from 50 to 350 °C with a heating rate of 2 °C/min. Here, the adsorbed NH_3 concentration was quantified from the peak area by calibration using the standard gas.

2. Results and discussion

2.1. Characterization of catalyst

N_2 sorption isotherms and pore size distributions of S-A catalysts with different weight ratios of chlorosulfonic acid to alumina (0:1, 1:1, 2:1, 3:1 and 4:1) are shown in Fig. S1. As obtained, the isotherm of S-A (0:1) exhibited the irreversible type IV sorption isotherm, corresponding to ordered mesoporous alumina material [28]. Here, the type H-2 hysteresis loops were appeared for all samples, suggesting to the ink-bottle mesoporous structure [29]. After alumina support was functionalized by sulfonic group with various adding amounts, the same isotherm such S-A (0:1) was found, indicating that the ordered mesoporous structure was well maintained. For porosity characteristic, narrow pore size distributions with a pore size range of 2.5 to 3.5 nm were established for all samples. Table 1 (in main paper) shows the textural properties including of surface area, pore volume and pore size of each catalyst. The surface areas and pore volume of S-A catalyst were reduced to some extent with the increasing in weight ratios of chlorosulfonic acid to alumina from 0:1 to 4:1. This should be clearly described to the dispersion of sulfonic group on catalyst surface and within porous structure. The increase in weight ratios of chlorosulfonic acid to alumina resulted in slight reduction of pore size, indicating that pore size of as-prepared catalyst did not obstruct by functionalization process in this work. It is possible that pristine mesoporous alumina prepared by Pluronic P123-assisted hydrothermal condition had high surface area and porosity so that why it could serve as an excellent support.

The XRD patterns of S-A catalysts with different weight ratios of chlorosulfonic acid to alumina are shown in Fig. S2. As shown in Fig. S2A, it is found that three diffraction peaks at 2.2, 3.8 and 4.4° was assigned to the (100), (110), and (200) planes, respectively, corresponding to a hexagonal mesoporous structure [30]. As obtained, the increasing in weight ratios of

chlorosulfonic acid to alumina from 0:1 to 4:1 resulted in slight reduction of peak intensities but no shifting of each peak which indicated that sulfonic group with additional amount had no effect for structural destruction of ordered-mesoporous alumina. As shown in Fig. S2B, the diffractogram of S-A (0:1) presented crystalline peaks around 32.6, 36.6, 39.5, 45.8, 60.6, and 67.2, which were attributed to the reflections on [220], [311], [222], [400], [511] and [440] crystal planes of the cubic gamma-alumina phase [31]. The intensity peaks were decreased to some extent with the increasing in weight ratios of chlorosulfonic acid to alumina, resulting from homogeneous covering by sulfonic group amount on catalyst structure. However, the ordered structure of gamma-alumina after sulfonic functionalization process was still retained since main crystalline peaks were appeared, suggesting that main structure did not remarkably destroy. A crystallite size range determined by Scherrer's equation was about 10.5 to 3.8 nm, obtaining from S-A (0:1) to S-A (4:1). The crystallite size of S-A (0:1) without sulfonic functionalization process was quite week, comparing with a commercial gamma-alumina. This should be resulted from structural modification by Pluronic P123, leading to enhancement of surface area and porosity of catalyst.

The SEM images of S-A (0:1) and S-A (3:1) are shown in Fig. S3a and b. One can see that the similar fiber-like morphologies with the uniform particle sizes were observed for both catalysts, indicating that their morphologies did not destroy during functionalization process. The possible way for formation of mesoporous fiber-like alumina are as follows: urea was applied as a reactant for controlling the precipitant condition. During synthesis process, urea was decomposed to ammonia and carbon dioxide, leading to the increasing of pH value in the system under thermal condition. They were then reacted with Al^{3+} to form ammonium aluminum carbonate hydroxide (AACH). In the assistance of Pluronic P123 surfactant, as a template, hydroxyl groups of AACH were further interacted on the micelles of Pluronic P123 via hydrogen bonding, leading to re-creation of new nucleus together with fiber-like particles

[32,33]. Here, excellent homogeneous dispersion of S element (sulfonic group) on the S-A structure was verified by EDX mapping image (Fig. S3). Fig. S3c and d shows the TEM images of S-A (0:1) and S-A (3:1). One can clearly see that the ordered mesoporous network aligned along the [110] and arranged along the [001] directions for both samples, revealing to the hexagonal mesoporous structure. This also confirms that ordered mesoporous alumina structure did destroy after sulfonic functionalization process. Also, the pore sizes evaluated by TEM analysis were found in the vicinity of ~3 nm. These results were in good agreement with BET and XRD results.

The existence of multiple functional groups on S-A catalyst was analyzed by FT-IR results (Fig. S4). The FT-IR spectra of both samples were displayed peaks at around 590 and 760 cm^{-1}, which could be attributed to the stretching vibrations of Al–O bond in S-A catalyst [34]. The stretching vibrations of O-H groups on the alumina surface and in the -SO$_3$H were found at around 3400 cm^{-1}. For S-A (3:1), the peaks at around 1045 and 1190 cm^{-1} were assigned to asymmetric and symmetric stretching modes of O=S=O/S-O stretching vibrations. This indicates that functionalization process of sulfonic group into mesoporous rod-like alumina structure was succeeded. The XPS results of S-A (3:1) are shown in Fig. S5. One can see that the catalyst consisted of Al, S and O was found without any impurities. The XPS spectrums exhibited a singlet Al 2p peak at binding energy of 74.4 eV with S 2p peak at binding energy of 168.8 eV, according to oxidation state of Al and sulfonic group in the S-A catalyst, respectively [35,36]. The XPS spectrum of O 1s peak was deconvoluted to two peaks according to O^{2-} bonded with Al^{3+} in alumina structure and oxygen involved sulfonic group, respectively. The thermal stability of S-A catalyst was studied by TGA analysis, and the result are shown in Fig. S6. One can see that weight loss at lower temperature of ~180 °C was be generally assigned for water evaporation from catalyst structure. The thermal decomposition of sulfonic group on catalyst was found with a significant reduction in the weight loss at the range of 350-550 °C. This

suggests that S-A catalyst had good thermal stability at lower temperature reaction of ~350 °C under oxygen condition, which was acceptable for GVL production process in this work.

References

[28]   L. Karam, M. Armandi, S. Casale, V. E. Khoury, B. Bonelli, P. Massiani, N. E. Hassan, Comprehensive study on the effect of magnesium loading over nickel-ordered mesoporous alumina for dry reforming of methane, *Energy Convers. Manage.*, 2020, 225, 113470.

[29]   S. Karnjanakom, A. Bayu, X. Hao, S. Kongparakul, C. Samart, A. Abudula, G. Guan, Selectively catalytic upgrading of bio-oil to aromatic hydrocarbons over Zn, Ce or Ni-doped mesoporous rod-like alumina catalysts, *J. Mol. Catal. A: Chem.*, 421 (2016) 235–244.

[30]   S. Karnjanakom, S. Kongparakul, C. Chaiya, P. Reubroycharoen, G. Guan, C. Samart, Biodiesel production from Hevea brasiliensis oil using SO_3H-MCM-41 catalyst, *J. Environ. Chem. Eng.*, 2016, 4, 47–55.

[31]   S. T. Bararpour, D. Karami, N. Mahinpey, Utilization of mesoporous alumina-based supports synthesized by a surfactant-assisted technique for post-combustion CO_2 capture, *J. Environ. Chem. Eng.*, 2021, 9, 105661.

[32]   Z. Tang, J. Liang, X. Li, J. Li, H. Guo, Y. Liu, C. Liu, Synthesis of flower-like Boehmite(γ-AlOOH) via a one-step ionic liquid-assisted hydrothermal route, *J. Solid State Chem.*, 2013, 202, 305–314.

[33]   X. Xu, Q. Yu, Z. Lv, J. Song, M. He, Synthesis of high-surface-area rod-like alumina materials with enhanced Cr(VI) removal efficiency, *Microporous Mesoporous Mater.*, 2018, 262, 140-147.

[34]   N. Ahmed, Z. N. Siddiqui, Mesoporous alumina sulphuric acid: A novel and efficient catalyst for on-water synthesis of functionalized 1,4-dihydropyridine derivatives via β-enaminones, *J. Mol. Catal. A: Chem.*, 2014, 394, 232–243.

[35]   D. Li, L. Ruan, J. Sun, C. Wu, Z. Yan, J. Lin, Q. Yan, Facile growth of aluminum oxide thin film by chemical liquid deposition and its application in devices, *Nanotechnol. Rev.*, 2020, 9, 876–885.

[36]   Z. Liu, Y. Qi, M. Gui, C. Feng, X. Wang, Y. Lei, Sulfonated carbon derived from the residue obtained after recovery of essential oil from the leaves of Cinnamomum longepaniculatum using Brønsted acid ionic liquid, and its use in the preparation of ellagic acid and gallic acid, *RSC Adv.*, 2019, 9, 5142–5150.
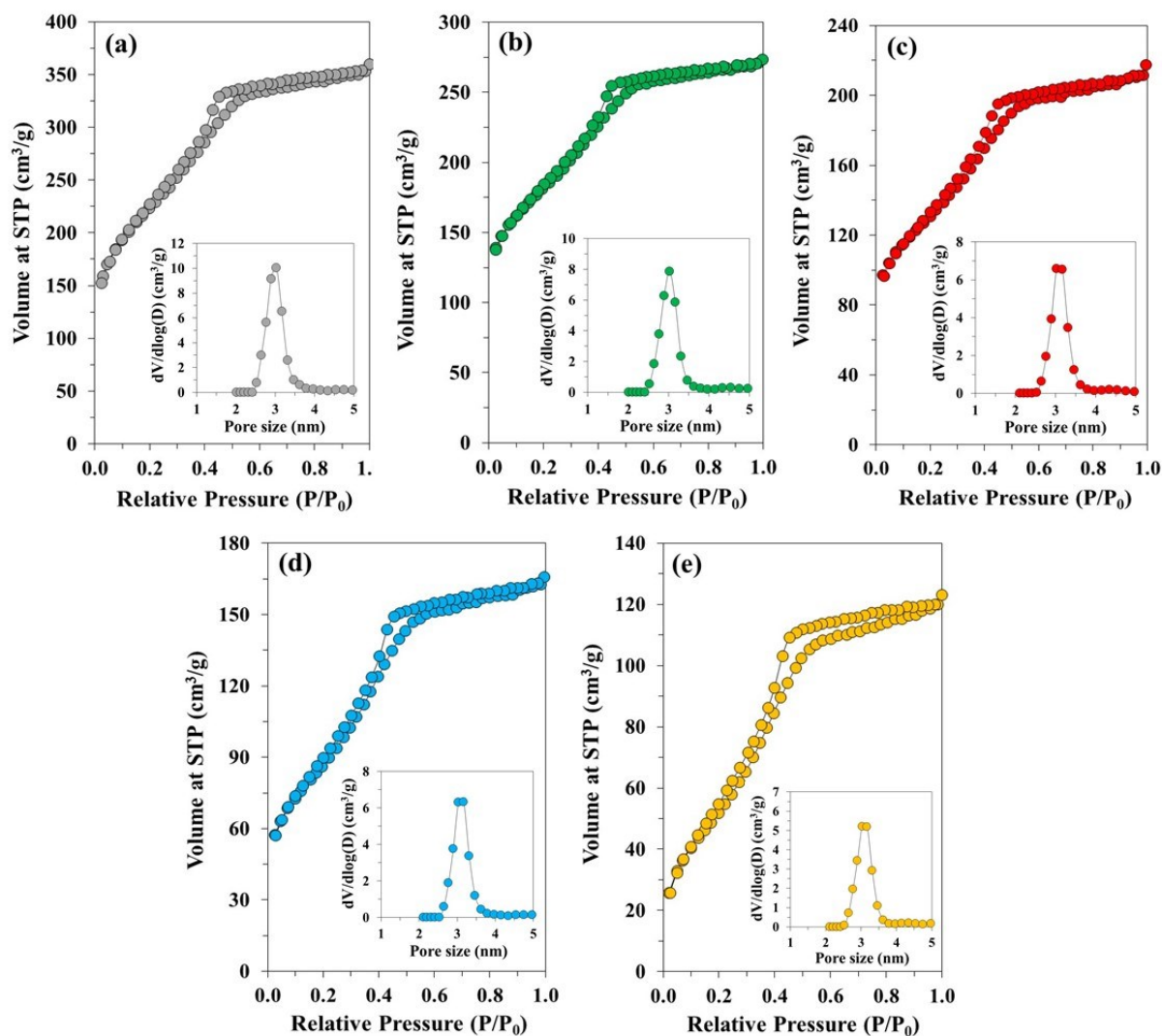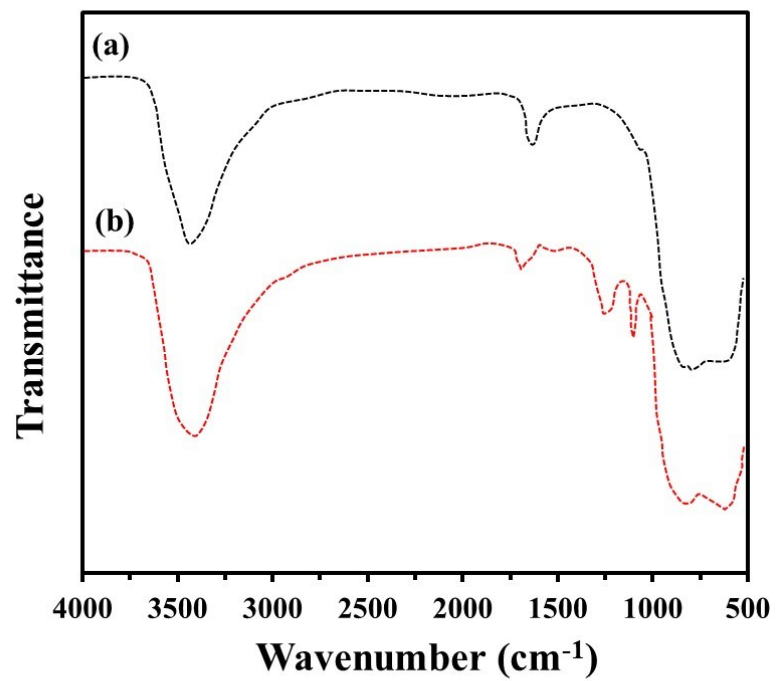
Fig. S1. N_2 sorption isotherms and pore size distributions of (a) S-A (0:1), (b) S-A (1:1), (c) S-A (2:1), (d) S-A (3:1) and (e) S-A (4:1).
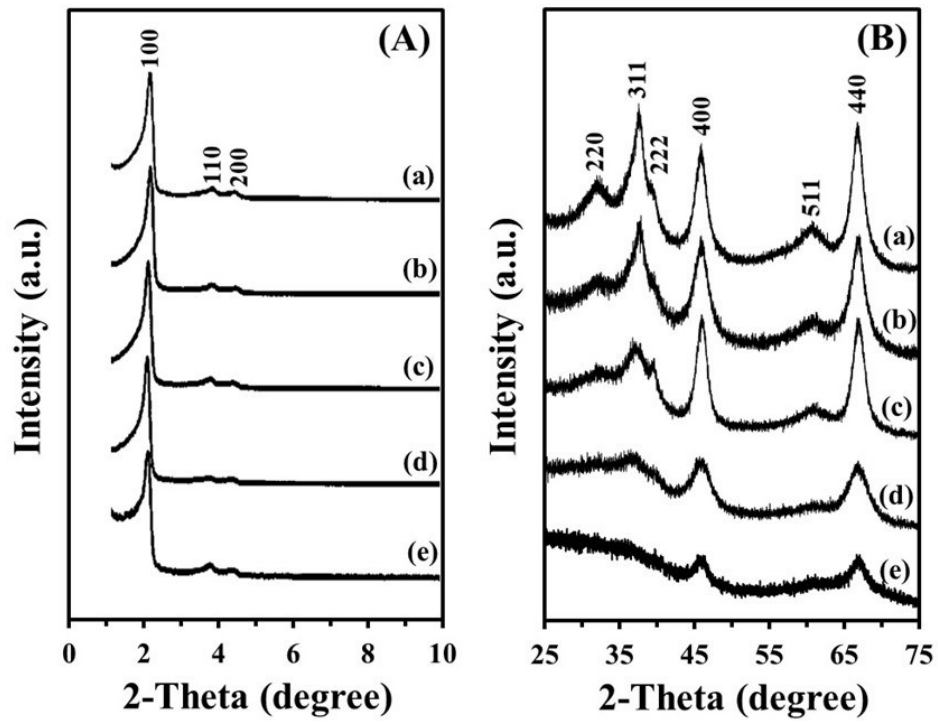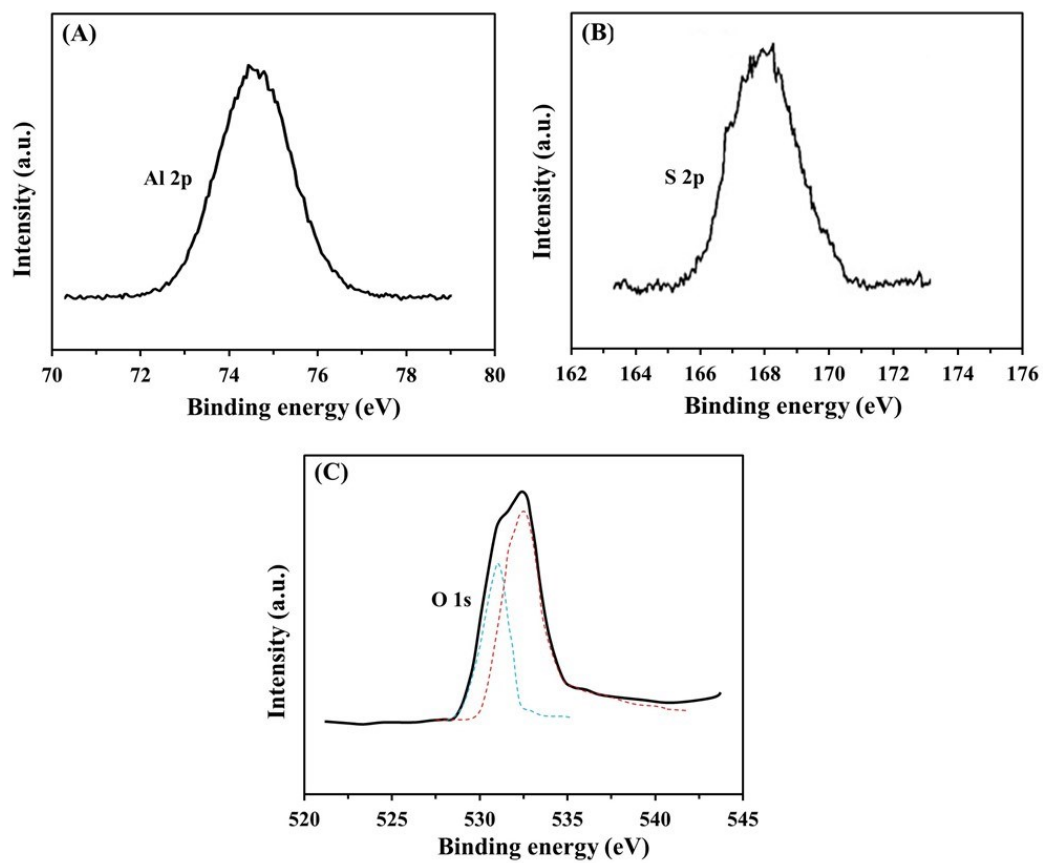
Fig. S2. XRD (small (A) and wide (B)-angle powders) patterns of (a) S-A (0:1), (b) S-A (1:1), (c) S-A (2:1), (d) S-A (3:1) and (e) S-A (4:1).
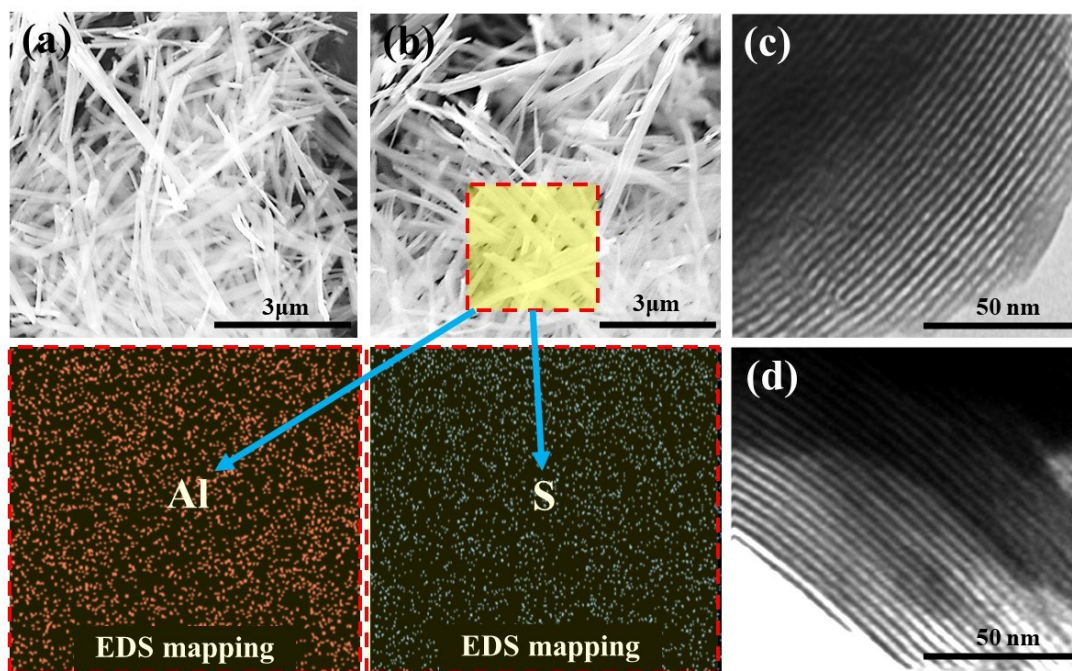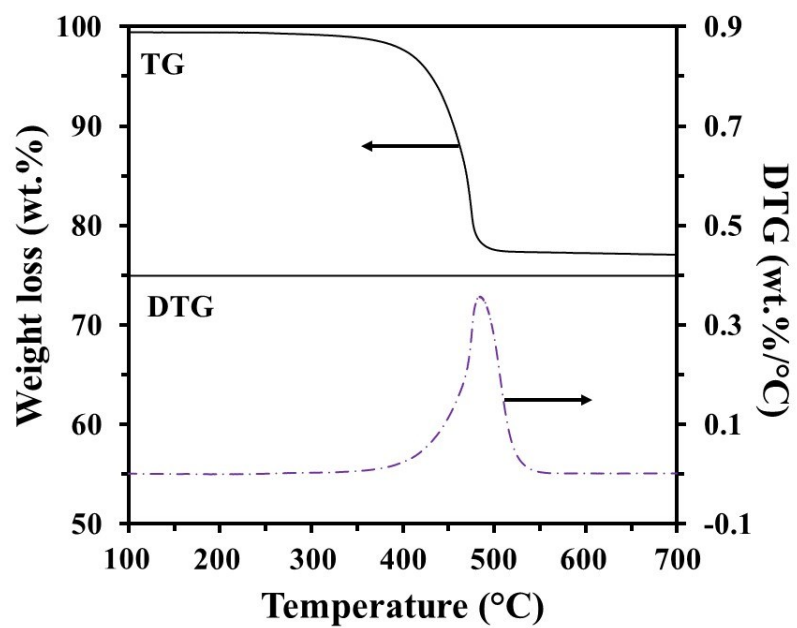
Fig. S3. SEM-EDS mapping images of (a) S-A (0:1) and (b) S-A (3:1). TEM images of (c) S-A (0:1) and (d) S-A (3:1)

Fig. S4. FTIR spectra of (a) S-A (0:1) and (b) S-A (3:1).

Fig. S5. XPS spectrum of (A) Al 2p, (B) S 2p and (C) O 1s of S-A (3:1).

Fig. S6. TG-DTG curves of S-A (3:1) at 100 to 700 °C under O_2 atmosphere.